Japanese Journal of Radiology (2024) 42:109–125
https://doi.org/10.1007/s11604-023-01493-0

INVITED REVIEW

Clinical and neuroimaging review of monogenic cerebral small vessel disease from the prenatal to adolescent developmental stage

Mikako Enokizono[1] · Ryo Kurokawa[2] · Akira Yagishita[3] · Yasuhiro Nakata[3] · Sho Koyasu[4] · Hiroshi Nihira[5] · Shigeko Kuwashima[6] · Noriko Aida[7] · Tatsuo Kono[1] · Harushi Mori[8]

Received: 12 September 2023 / Accepted: 15 September 2023 / Published online: 17 October 2023

Abstract

Cerebral small vessel disease (cSVD) refers to a group of pathological processes with various etiologies affecting the small vessels of the brain. Most cases are sporadic, with age-related and hypertension-related sSVD and cerebral amyloid angiopathy being the most prevalent forms. Monogenic cSVD accounts for up to 5% of causes of stroke. Several causative genes have been identified. Sporadic cSVD has been widely studied whereas monogenic cSVD is still poorly characterized and understood. The majority of cases of both the sporadic and monogenic types, including cerebral autosomal-dominant arteriopathy with subcortical infarcts and leukoencephalopathy (CADASIL), typically have their onset in adulthood. Types of cSVD with infantile and childhood onset are rare, and their diagnosis is often challenging. The present review discusses the clinical and neuroimaging findings of monogenic cSVD from the prenatal to adolescent period of development. Early diagnosis is crucial to enabling timely interventions and family counseling.

Keywords Cerebral small vessel disease · Monogenic · Hereditary · Pediatric · Cerebral calcification

Introduction

Cerebral small vessels consist of two components: first, the vasoganglion deriving from the leptomeninges covering the subarachnoid space and the convex surface of the brain; and second, perforating arteries originating in the anterior, middle, and posterior cerebral arteries, which supply the subcortical parenchyma. Cerebral small vessels are essential for maintaining adequate blood flow to the subsurface brain structures [1].

Cerebral small vessel disease (cSVD) refers to a group of pathological processes with various etiologies affecting the small vessels of the brain, including small arteries and arterioles but also capillaries and venules [2], which are commonly 50–400 mm in length [1]. To understand better the pathogenesis of cSVD, it is necessary to consider how capillary endothelial cells and pericytes interact with astrocytes, oligodendrocytes, and microglia, which comprise the neuroglio-vascular unit, where cells interact to regulate the entry of fluid and nutrients into the interstitium, manage blood supply, maintain and repair myelin, clear fluid and waste, and maintain the interstitial milieu for appropriate cell function [3]. Neuro-glio-vascular unit dysfunction plays a key role in the initiation and progression of cSVD.

✉ Mikako Enokizono
mikako_enokizono@tmhp.jp

1 Department of Radiology, Tokyo Metropolitan Children's Medical Center, 2-8-29 Musashidai, Fuchu, Tokyo 183-8561, Japan

2 Department of Radiology, Graduate School of Medicine, The University of Tokyo, Bunkyo-ku, Tokyo, Japan

3 Department of Neuroradiology, Tokyo Metropolitan Neurological Hospital, Fuchu, Tokyo, Japan

4 Department of Diagnostic Imaging and Nuclear Medicine, Kyoto University, Sakyo-ku, Kyoto, Japan

5 Department of Pediatrics, Kyoto University, Sakyo-ku, Kyoto, Japan

6 Department of Radiology, Dokkyo Medical University, Shimotsuga-gun, Tochigi, Japan

7 Department of Radiology, Kanagawa Children's Medical Center, Yokohama, Kanagawa, Japan

8 Department of Radiology, School of Medicine, Jichi Medical University, Shimotsuke, Tochigi, Japan

Several manifestations of cSVD have been identified in humans, including blood–brain barrier (BBB) dysfunction, impaired vasodilation, vessel stiffening, dysfunctional blood flow, interstitial fluid drainage, white matter rarefaction, ischemia, inflammation, myelin damage, and secondary neurodegeneration in global brain effects [4–7]. Many affected individuals exhibit no symptoms in the early stages of this condition, but brain damage can result in sudden-onset stroke, cognitive decline, dementia, gait and balance problems, sphincter dysfunction, and psychiatric disorders [8, 9].

The neuroimaging features of cSVD include small, subcortical infarcts, lacunar infarcts, white matter hyperintensities, enlargement of perivascular spaces, microbleeds, superficial siderosis, large hemorrhages, calcification, and brain atrophy [2, 3, 10]. Because small vessels cannot currently be visualized in vivo, the term, small vessel disease is frequently used to describe parenchymal lesions rather than the underlying small vessel alterations. Sensitive MRI techniques can reveal pathological alterations occurring in the so-called normal-appearing white and gray matter [4, 5].

Pantoni has classified cSVD into the following categories according to pathological cerebrovascular changes [2]: Type 1, arteriolosclerosis (or age-related and vascular risk factor-related small vessel diseases); Type 2, sporadic and hereditary cerebral amyloid angiopathy (CAA); Type 3, inherited or genetic small vessel diseases distinct from cerebral amyloid angiopathy; Type 4, inflammatory and immunologically mediated small vessel diseases; Type 5, venous collagenosis; and Type 6, other small vessel diseases, such as post-radiation angiopathy. These various, pathological changes result in damage to the brain parenchyma, including neuronal apoptosis, diffuse axonal injury, demyelination, and loss of oligodendrocytes.

Most cases of cSVD are sporadic, with the age-related and hypertension-related types and CAA being the most prevalent forms. Monogenic cSVD accounts for up to 5% of all causes of stroke [11]. Several causative genes have been identified [12–15]. Monogenic cSVD, the most common type, is an autosomal-dominant, cerebral arteriopathy characterized by subcortical infarcts and leukoencephalopathy (CADASIL) arising from *NOTCH3* gene mutations [16]. Sporadic cSVD has been widely studied whereas monogenic cSVD is still poorly characterized and understood. The majority of cases of both the sporadic and monogenic types, including CADASIL, typically have their onset in adulthood. Forms of the disease manifesting in infancy and childhood are rare, and their diagnosis is often challenging.

The present review discusses the clinical and neuroimaging findings of monogenic cSVD, which occurs from the prenatal to adolescent period of development.

Prenatal period

COL4A1/COL4A2-related disorders

COL4A1 and *COL4A2*, both located on chromosome 13q34, encode the alpha1 and alpha 2 chains of type IV collagen, a key component of basement membranes in blood vessels and various soft organs in mammals [17]. Mutations in these genes can give rise to brain small vessel disease 1 (BSVD1, OMIM#175,780) and 2 (BSVD2, OMIM#614,483), respectively, and have been associated with a broad spectrum of cerebrovascular, renal, ophthalmological, cardiac, and muscular abnormalities known as *COL4A1/COL4A2*–related disorders. They are inherited in an autosomal dominant (AD) fashion and have a high, de novo mutation rate. This complex of disorders is characterized by highly incomplete penetrance and a wide range of phenotypic variation even among family members [18] and manifest at any developmental stage, from the prenatal (fetal) to the adult stage.

Cerebrovascular manifestations occur in more than half of individuals harboring a *COL4A1* mutation [14]. *COL4A2* mutations are apparently associated with even less penetrance and a globally milder phenotype than *COL4A1* mutations [19]. Seizures are the most prevalent clinical symptom associated with these variants. Motor dysfunction and developmental delay are highly prevalent [18].

Prenatal and neonatal intracerebral hemorrhage (ICH) and encephaloclastic porencephaly are frequently associated with mutations in both *COL4A1* and *COL4A2* [18, 20–22]. Their most common cause is a germinal matrix hemorrhage leading to deep venous infarction involving the basal ganglia and frontal lobe, tissue necrosis, and porencephalic cavitation (Fig. 1). Prenatal ICH size correlates clinically with motor outcomes [22]. Extensive bilateral porencephaly also resembles hydranencephaly.

Schizencephaly, also known as dysplastic porencephaly, is defined as a cleft extending from the pial surface to the lateral ventricle and lined by heterotopic gray matter. Schizencephaly is also associated with mutations in *COL4A1* and *COL4A2* [23, 24]. Niwa et al. reported susceptibility-weighted imaging (SWI) findings demonstrating hemorrhages in the peripheral portion of the schizencephalic and intraparenchymal region. Venous tortuosity may be helpful in assessing for a possible relationship between schizencephaly and *COL4A1* mutations [25]. Other cortical malformations, ranging from polymicrogyria to subependymal and subcortical heterotopia without hemorrhage or calcification, have also been reported [24].

Other types of brain lesion related to prenatal hemorrhage have been reported in mutations in children, such as

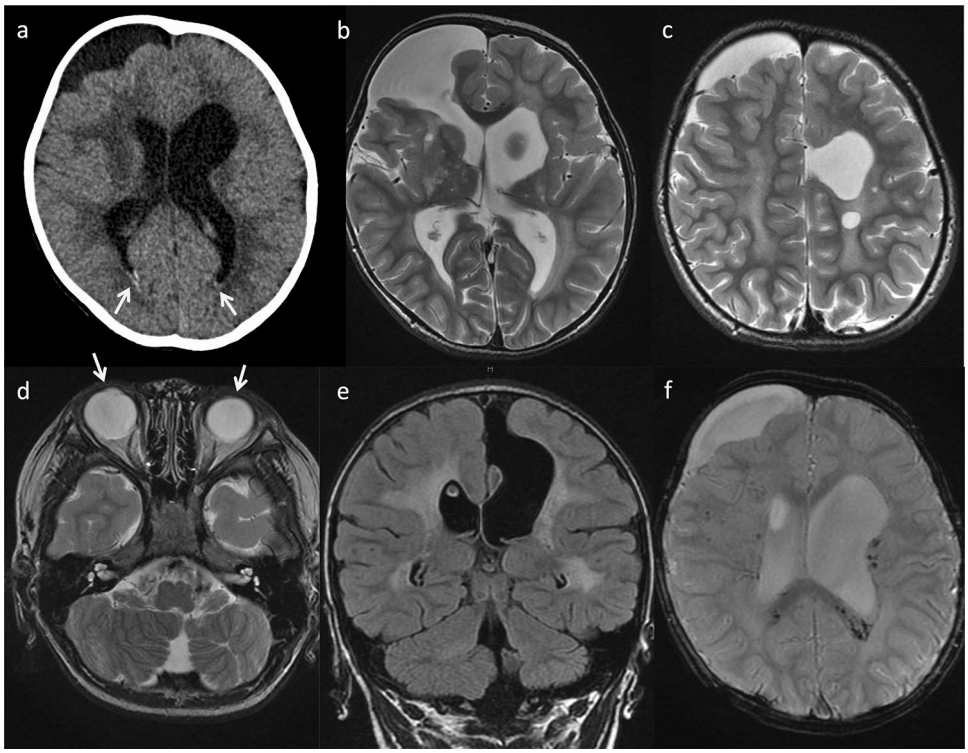

Fig. 1 A 3-year-old, male patient with *COL4A1*-related disorder. **a** Axial non-contrast computed tomography demonstrated calcification along the bilateral occipital horns of the lateral ventricles (arrows) and asymmetrical ventricular enlargement. **b-e** Axial T2-weighted imaging and coronal FLAIR imaging revealed porencephaly in the bilateral frontal lobes, asymmetrical ventricular enlargement, hyperintensities in the bilateral basal ganglia, thalami, deep white matter, and cerebellar dysplasia. Note also the implanted intraocular lens for cataracts (arrows). **f** Axial T2*-weighted imaging demonstrated multiple microbleeds in the splenium of the corpus callosum and subcortical and deep white matter

abnormal basal ganglia, dysplastic brain stem, cerebellar hemorrhage, cerebellar hypoplasia/atrophy, brain calcification, ventricular asymmetry, mild ventriculomegaly, and hydrocephalus (Figs. 1, 2) [18, 26, 27] while Dandy-Walker malformation may occur prenatally [28].

Periventricular leukomalacia (PVL), defined as pre- or perinatal, post-hypoxic-ischemic leukoencephalopathy without porencephaly is reported in *COL4A1* mutations [18]. In the absence of a remarkable family history, this PVL phenotype may elude diagnosis. In the absence of other prominent symptoms, such as porencephaly, a high creatine kinase (CK) concentration or microbleeds may be helpful in diagnosing this PVL phenotype in *COL4A1* mutations.

MR angiography can also detect asymptomatic, intracranial aneurysms, dolichoectasia, and vascular tortuosity. These most frequently occur in the internal carotid arteries, specifically in the C4 and C5 segments. In certain instances, they can affect the basilar artery as well [29].

A distinct phenotype known as hereditary angiopathy, nephropathy, aneurysms, and cramps (HANAC) stems from *COL4A1* mutations at exons 24 and 25 [30]. The cerebrovascular phenotype is characterized by cSVD with a low risk of hemorrhagic stroke and the presence of aneurysms around the carotid siphon. Bilateral retinal arteriolar tortuosity is persistent and frequently accompanied by multiple, retinal hemorrhages in the absence of any other ocular abnormality. Patients with HANAC may also experience muscle spasms and kidney lesions, which can contribute to renal cyst formation, chronic kidney failure, and occasionally hematuria.

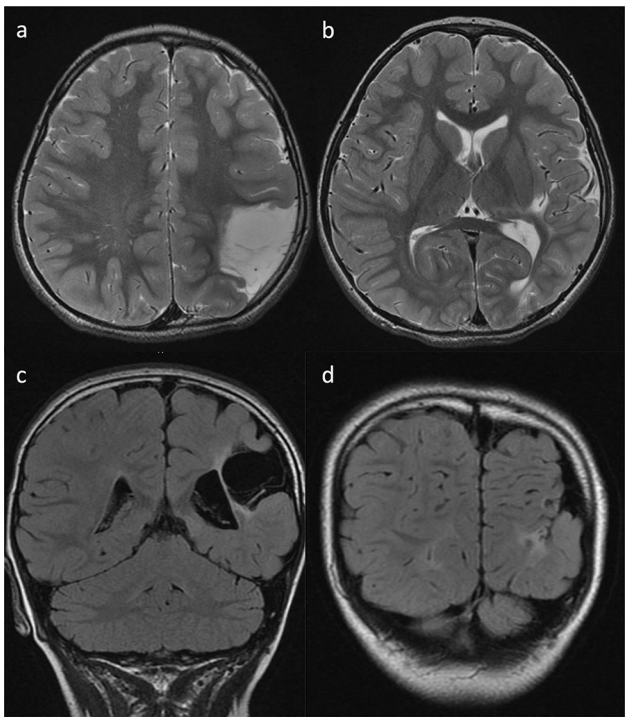

Fig. 2 *COL4A2*-related disorder in a 5-year-old, male patient with right hemiparesis. Axial T2-weighted imaging (**a**, **b**) and coronal FLAIR imaging (**c**, **d**) demonstrated cystic encephalomalacia in the left parietal lobe, ulegyria in the left insula and occipital lobe, and hyperintensities in the left posterior limb of the internal capsule and thalamus

There is no effective treatment. However, patients and their physicians should be informed that the fragility of the vascular wall may lead to a cerebral or retinal hemorrhage, which can cause the vascular wall to rupture in response to trauma (shock, vigorous physical movement, vaginal delivery) or anticoagulant use, which individuals with this condition should avoid [31]. In pregnant patients with this condition, cesarean delivery has been proposed as a method of avoiding birth trauma to prevent cerebral vascular injury [32].

Similarly, dysfunction of the tight junction components, such as occludin (OCLN) and junctional adhesion molecules (JAMs), is associated with overlapping clinical presentations. In particular, *JAM3* mutations are known to cause congenital cataracts and hemorrhagic destruction of the brain [33, 34]. *JAM3* screening should be requested in prenatal diagnostic screening for congenital cataracts.

COLGALT1-related disorders

COLGALT1-related disorders (BSVD3, OMIM #618,360) are autosomal recessive disorders caused by mutations in the *COLGALT1* gene on chromosome 19p13, which encodes the collagen beta galactosyltransferase 1 (ColGalT1) protein. ColGalT1 initiates glycosylation of CoL4a1 (and possibly Col4a2), a crucial step in the formation of the triple helix of collagen IV. Miyatake et al. [35] described two patients with a compound heterozygous variant of the *COLGALT1* gene and demonstrated that decreased ColGalT1 activity leads to decreased synthesis of CoL4a1 protein, thereby reducing type IV collagen secretion. Additionally, Teunissen et al. reported a more severe phenotype with a homozygous essential splice site variant of the *COLGALT1* gene [36].

The resulting phenotype varies highly in terms of the timing and location of intracranial hemorrhages. Some patients may have in utero or early infantile onset accompanied by severe, global, developmental delay, spasticity, and seizures and require full support for daily living. Other patients may exhibit normal or mildly delayed development accompanied by a sudden onset of intracranial hemorrhage resulting in acute, neurological decline. Environmental stress (either in utero stress or an infection) might trigger its onset, as is the case in *COL4A1/COL4A2*-related disease.

The radiographic features of *COLGALT1*-related disorders are also comparable to those of *COL4A1/COL4A2*-related disease [35, 36]. MRI findings typical of *COL4A1/COL4A2*-related disease include porencephaly, parenchymal/intraventricular hemorrhage, hydrocephalus, cerebral calcification, microbleeds, vascular leukoencephalopathy, lacunar infarcts, dilated perivascular spaces, and intracranial aneurysms (Figs. 3, 4).

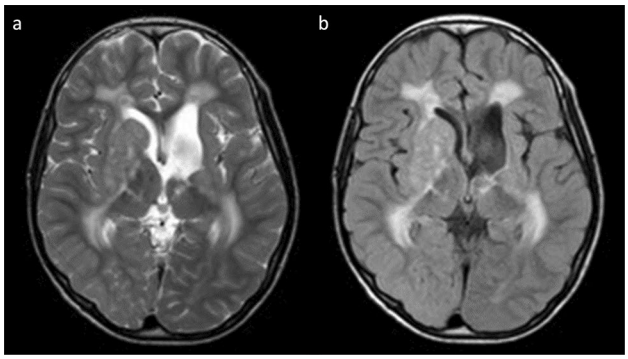

Fig. 3 *COLGALT1*-related disorder in a 12-year-old, male patient with severe developmental delay, epilepsy, spastic quadriplegia. Axial T2-weighted imaging (**a**) and FLAIR imaging (**b**) demonstrated porencephaly in the left hemisphere with destructive changes of the basal ganglia and bilateral leukoencephalopathy with mild atrophy. Hyperintense lesions were also observed in the right basal ganglia, posterior limb of the internal capsule, and bilateral thalami (reprinted with permission from Reference [35])

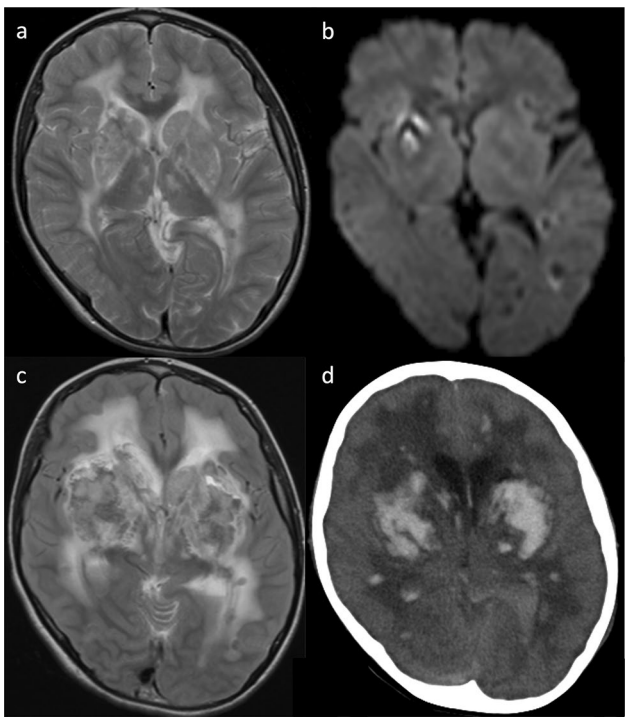

Fig. 4 *COLGALT1*-related disorder. Axial T2-weighted imaging (**a**) at the age of 9 years demonstrated hyperintense lesions in the bilateral basal ganglia, thalami, deep cerebral white matter, and internal and external capsules. Axial diffusion-weighted imaging (DWI) (**b**) revealed susceptibility effects of microbleeds in the right basal ganglia and left temporal white matter. After 1 day, axial FLAIR imaging (**c**) and computed tomography (**d**) after the patient lost consciousness owing to an influenza virus infection demonstrated acute, massive, bilateral, parenchymal and intraventricular hemorrhages (reprinted with permission from Reference [35])

Neonatal and infantile stages

Incontinentia pigmenti

Incontinentia pigmenti (IP, also called Bloch-Sulzberger syndrome, OMIM #308,300) is an X-linked, neurocutaneous disorder caused by a mutation in the IKK-gamma gene (*IKBKG*), also called *NEMO*, on chromosome Xq28. *IKBKG* is essential for the activation of the nuclear factor-kappa B (NF- κB) transcription factor, which is involved in preventing tumor necrosis factor-alpha (TNF-α)-induced apoptosis and in regulating the immune and inflammatory responses [37]. Thus, *IKBKG*-deficient cells are probably more prone to inflammation and apoptosis. IP is characterized by congenital skin lesions, dental and skeletal dysplasia, and ocular and central nervous system (CNS) abnormalities. IP is almost exclusively seen in females. The mutations appear to be lethal in males; postzygotic mosaicism related to *IKBKG* has been reported in only a few male patients [38].

The skin lesions characteristic of IP progress through the bullous stage (birth to age 4 months); the verrucous stage (for several months); the hyperpigmentation stage (age 6 months to adulthood); to the atretic stage. The skin abnormalities characterizing each stage occur along the lines of embryonic and fetal skin development known as the Blaschko lines [39, 40] (Fig. 5), which correspond to cell migration or growth pathways established during embryogenesis. Similar to dermatomes, they are linear at the extremities and circumferential at the trunk.

Neurological manifestations occur in 30% of IP patients, constituting one of the major causes of morbidity and mortality associated with the condition. Symptoms, such as seizures, intellectual disability, developmental delay, spastic paresis, cerebellar ataxia, and microcephaly, may also be observed. Most neurological features occur from the neonatal through the early infantile period and only rarely in late childhood [41, 42]. Inflammatory mechanisms, vascular injury, and possibly disturbed apoptosis during development are apparently at the root of the cerebral manifestations [43].

Brain MRI can visualize tissue damage resulting from disease in small vessels as well as also medium-sized cerebral arteries [44]. Such tissue damage may include periventricular and subcortical white matter disease, hemorrhagic changes, corpus callosum hypoplasia, polymicrogyria, cortical dysplasia, cerebral atrophy, cerebellar hypoplasia, myelination delays or ventricular dilatation [43, 45]. DWI abnormalities are characteristic, with multifocal and punctate lesions distributed throughout the white matter in a speckled pattern often associated with changes in the corpus callosum. Reduced diffusion is also observed in the basal ganglia, thalami, cerebellum, and cerebral peduncles [40, 46] (Fig. 5). Sequential scans in affected infants demonstrate progressive cortical and white matter cavitation/atrophy, ventricular enlargement, and thinning of the corpus callosum.

Ocular abnormalities are another major cause of disability in IP patients. Approximately 20–37% of IP patients have an ocular defect, such as strabismus, retinopathy, congenital cataract or microphthalmia [47, 48].

Previous studies have reported retinal lesions and perivascular and intravascular eosinophilic infiltration of the CNS and skin in IP. Maingay-de Groof et al. reported that *NEMO* mutation activates eotaxin, a potent, eosinophil-selective chemokine that is highly expressed by endothelial cells in IP and correlates with perivascular and intravascular eosinophilic infiltration [44].

Aicardi-Goutieres syndrome

Aicardi-Goutieres syndrome (AGS) typically manifests as an early-onset, subacute encephalopathy usually resulting in profound intellectual and physical disability. AGS presents at birth or in the first few weeks of life with abnormal neurological findings, hepatosplenomegaly, elevated liver enzymes, and thrombocytopenia. Although AGS is phenotypically similar to congenital toxoplasmosis, other, rubella, cytomegalovirus, herpes simplex (TORCH) infections, serological tests for common prenatal infections return negative. Over time, chilblain skin lesions on the fingers, toes, and ears develop in up to 40% of individuals. Severe, neurological dysfunction becomes clinically apparent in infancy, manifesting as progressive microcephaly, spasticity, dystonic posturing, and profound psychomotor retardation, often leading to death in early childhood. Recently, atypical, sometimes milder, cases of AGS have come to light [49].

Many, previous studies have advocated the use of the more generic term, type I interferonopathy (IFN), to refer to this group of monogenic diseases because the upregulation of type I interferon is a crucial aspect of its pathogenesis [50]. Mutations in any of the following nine genes may result in the AGS phenotype: *TREX1* (AGS1, OMIM #225,750), *RNASEH2B* (AGS2, OMIM #610,181), *RNASEH2C* (AGS3, OMIM #610,329), *RNASEH2A* (AGS4, OMIM #606,034), *SAMHD1* (AGS5, OMIM #612,952), *ADAR* (AGS6, OMIM #615,010), *IFIH1* (AGS7, OMIM #615,846), *LSM11* (AGS8, OMIM #619,486), and *RNU7-1* (AGS9, OMIM #619,487). The encoded proteins are involved in nucleic acid metabolism and/or signaling. Spinal fluid and serum analysis reveals elevated levels of interferon activity stemming from increased expression of interferon-stimulated genes in the peripheral blood [51]. *TREX1* mutations are associated with a true neonatal presentation [52]. Most patients present symptoms at a slighter later age. Mutations most frequently occur in *RNASEH2B* [53].

Computed tomography (CT) demonstrates multiple, punctate or globular calcifications of the basal ganglia,

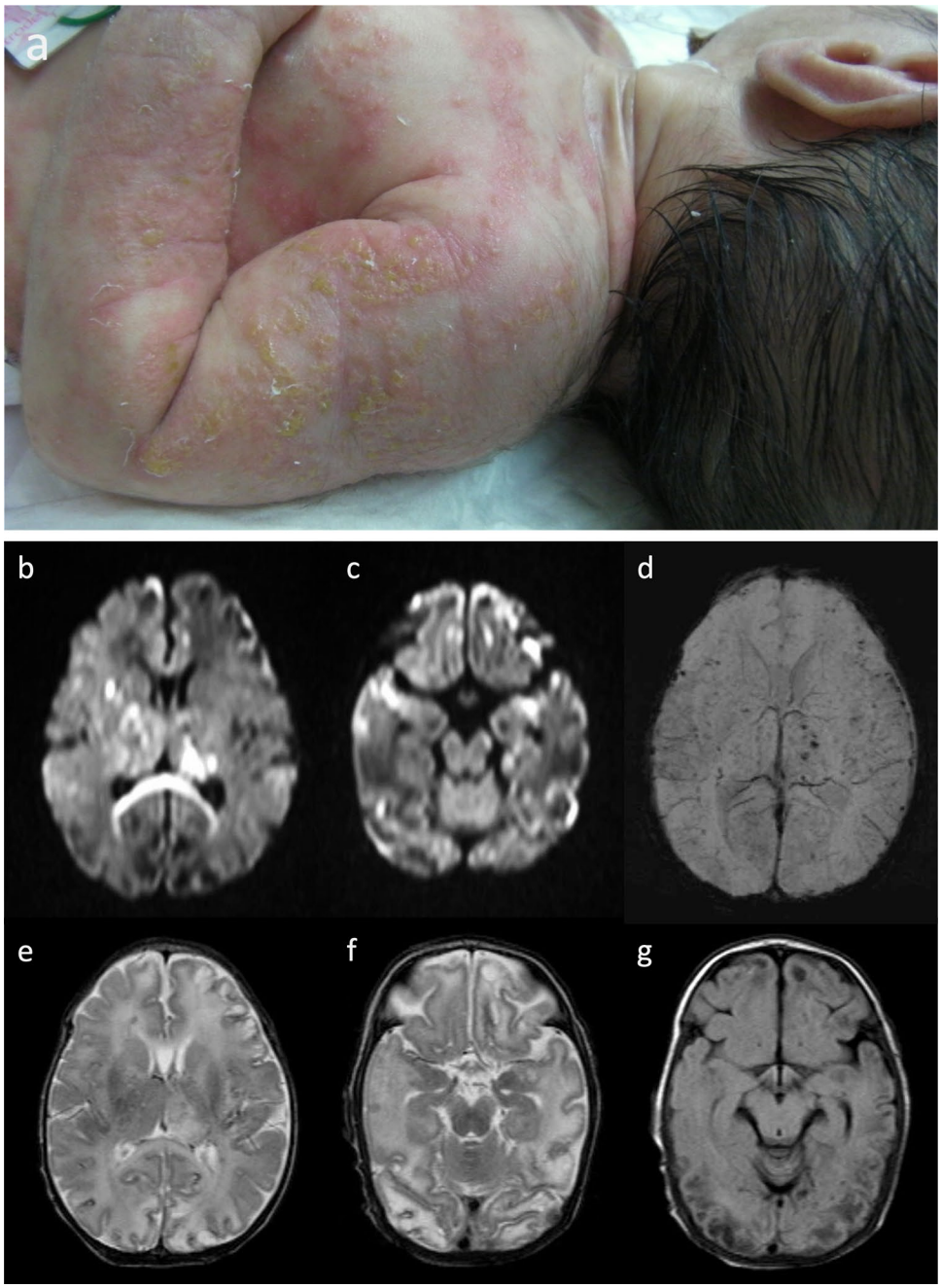

Fig. 5 Incontinentia pigmenti in a female neonate with a decreased level of consciousness and weak sucking reflex. **a** A clinical photograph of skin lesions on day 15 shows an erythematous and vesiculobullous rash on her arms and trunk spreading in along the Blaschko lines (reprinted with permission from Reference [40]). **b**, **c** Axial DWI demonstrated multiple areas of ischemic change with scattered foci of restricted diffusion in the bilateral cerebral cortices, basal ganglia, thalami, splenium of the corpus callosum, and midbrain. (**d**) Axial susceptibility-weighted imaging (SWI) demonstrated multiple microhemorrhages in the bilateral cerebral cortices and thalami. **e, f** Axial T2-weighted imaging and FLAIR imaging (**g**) found multiple, cavitary lesions in the bilateral, cerebral subcortical white matter

particularly the putamina, thalami, deep and subcortical white matter, and cerebellar dentate nuclei (Fig. 6). *TREX1* mutations tend to produce particularly severe calcification [53]. T2-weighted imaging demonstrates hyperintensity in the subcortical and deep white matter, especially in the frontal and temporal lobes [49]. White matter rarefaction and anterior temporal lobe cysts are strongly associated with *TREX1* mutations and early age at onset [53, 54].

Cerebral atrophy is usually progressive, and cerebellar atrophy and brain stem atrophy are prevalent. Delayed myelination is associated with *RNASEH2B* mutations and early age at onset [53]. Intracerebral vasculopathy, including intracranial stenosis, moyamoya syndrome, and aneurysms, is associated with *SAMHD1* mutations [55] while bilateral striatal necrosis is associated with *ADAR* mutations [56]. RNASET2-deficient leukoencephalopathy mimics AGS and congenital cytomegalovirus infection clinically and radiologically [57].

Despite the lack of an established treatment, immune modulation (such as corticosteroid therapy) during the active phase may be beneficial [49]. Janus kinase (JAK) inhibitors are reportedly beneficial in controlling inflammation and

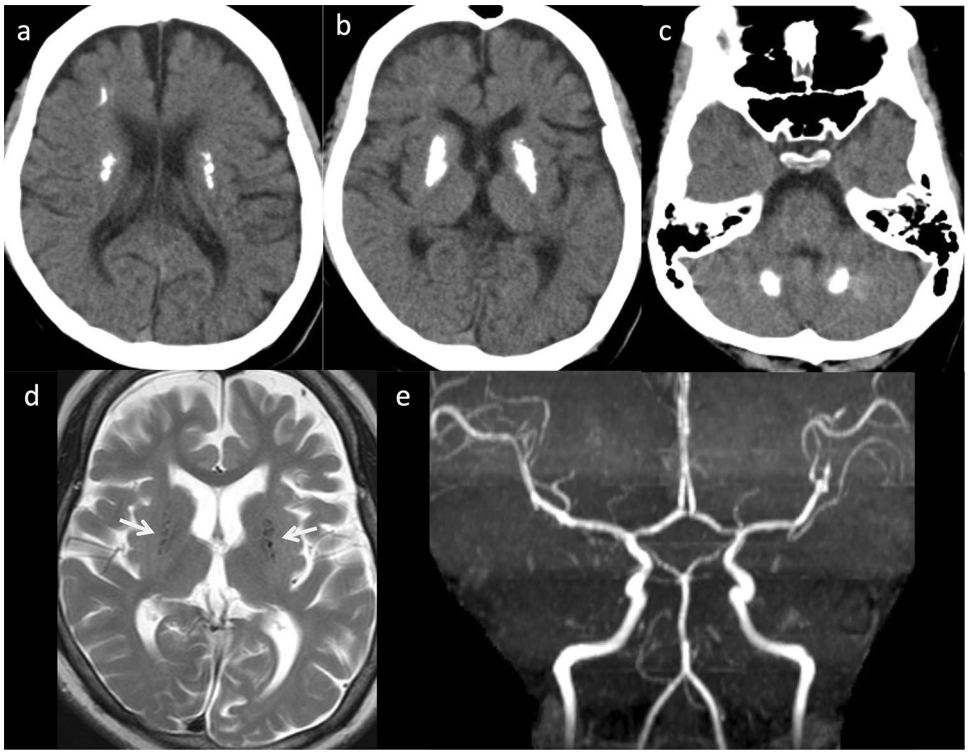

Fig. 6 Aicardi-Goutieres syndrome with *IFIH1* mutations in a 15-year-old, female patient with quadriplegia and chilblain skin lesion of the big toe. **a–c** Axial non-contrast computed tomography found multiple calcifications of the bilateral, right frontal, subcortical white matter, bilateral deep white matter, basal ganglia, and cerebellar dentate nuclei. **d** Axial T2-weighted imaging demonstrated mild cerebral atrophy. The bilateral basal ganglia demonstrated a few, punctate hypointensities secondary to calcification (arrows). **e** MR angiography revealed mild stenosis of the major cerebral arteries

preventing the progression of end-organ damage by blocking interferon activation in type 1 interferonopathies, including AGS [58, 59].

Childhood and adolescence

Mitochondrial encephalomyopathy with lactic acidosis and stroke-like episodes (MELAS)

Mitochondrial encephalomyopathy with lactic acidosis and stroke-like episodes (MELAS, OMIM #540,000) refers to a heterogeneous group of disorders caused by point mutations in mitochondrial DNA. The majority of patients have in common the pathogenic variant m.3243A > G in the mitochondrial DNA tRNA-leucine (MT-TL1) [60] and may experience the onset of symptoms, including headache, nausea, seizures, episodic vomiting, and permanent or reversible stroke-like episodes as well as some symptoms of generalized mitochondrial disease, at any age (the second decade is the most common). Compared to strokes of vascular origin, there is a higher incidence of clinical symptoms, such as cortical blindness and auditory agnosia [31]. Serum and CSF lactate are usually elevated at the time of presentation.

Although the underlying, pathophysiological mechanism of the stroke-like episodes remains unclear, the cytopathic and angiopathic theories are two, prevailing hypotheses of their etiology [61]. The cytopathic theory proposes that defects in oxidative phosphorylation resulting from mitochondrial mutation cause neuronal and glial cellular dysfunction, potentially resulting in cell death during periods of increased metabolic activity. The angiopathic theory proposes that abnormal mitochondrial function in the arteriolar endothelium leads to impaired autoregulation and ischemia.

Brain CT demonstrates symmetrical calcification in the basal ganglia more prominently in older patients [62]. MRI findings of stroke-like lesions do not correspond to vascular territories, involve the cortex and juxtacortical white matter, and primarily affect the parietal and occipital lobes and basal ganglia (Fig. 7). Some studies have reported decreased diffusion in some affected areas [63, 64] while other studies have reported the opposite [65]. Sequential scans may reveal the resolution and subsequent reappearance of abnormal areas or the development of new lesions. Most of the severe lesions progress to cortical laminar necrosis, gliosis, and atrophy [66].

^{1}H-MR spectroscopy (MRS) demonstrates a high lactate level in the affected areas of the brain (Fig. 7). The presence of lactate in areas of the brain that are not visibly abnormal on T2 or diffusion imaging is more suggestive of mitochondrial disease [67, 68]. MR angiography reveals prominent dilatation of the arteries (Fig. 7), and perfusion-weighted imaging (PWI) and arterial spin labeling (ASL) demonstrate hyperperfusion in the affected areas in the acute stage, which may be useful in differentiating MELAS from acute ischemic stroke [69, 70]. In the chronic phase, PWI and ASL show hypo- or iso-perfusion in the affected areas [68]. Moreover, regional hyperperfusion has also been revealed on

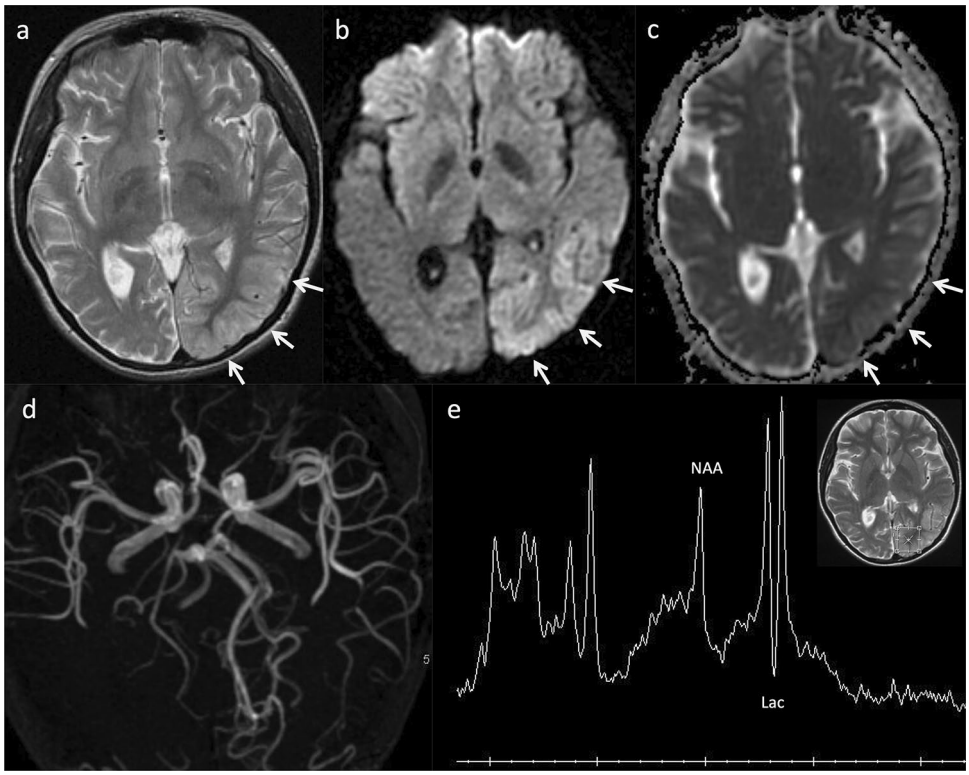

Fig. 7 MELAS with point mutations of m.3243A > G in the mitochondrial DNA tRNA-leucine (MT-TL1) in a 10-year-old, female patient with transient visual impairment. Axial T2-weighted imaging (**a**) demonstrated mild swelling and hyperintensity in the left temporal and posterior cortices (arrows). Axial DWI (**b**) demonstrated hyperintensity in the left temporal and posterior regions, and an ADC map (**c**) demonstrated corresponding, increased diffusion (arrows). MR angiography (**d**) revealed dilation of the left middle and posterior cerebral arteries. ^{1}H-MRS (PRESS, TE/TR 35/2,000 ms) (**e**) of the left occipital lobe revealed a prominent doublet peak of lactate and decreased NAA/Cr ratio. *MELAS* mitochondrial encephalomyopathy with lactic acidosis and stroke-like episodes, *PRESS* point-resolved spectroscopy, *NAA* N-acetyl aspartate

ASL during the preclinical phase three to 5 months before the clinical onset of stroke-like episodes [71].

Fabry disease

Fabry disease (FD, OMIM #301,500) is the most prevalent lysosomal storage disorder and is caused by mutations in the *GLA* gene on chromosome Xq22 encoding alpha-galactosidase A (α-GalA). This enzymatic defect leads to abnormal accumulation of globotriaosylceramide (Gb3) in various organ systems, especially vascular endothelial and smooth muscle cells [72]. Renal failure, cardiomyopathy, and CNS alterations are the main causes of morbidity and reduced life expectancy in patients with this disease. Although FD was previously considered to be an X-linked recessive disorder, female patients with heterozygous genetic involvement are known to have a spectrum of presentations ranging from the asymptomatic to the severe. Neonatal screening has detected an unexpectedly high prevalence of this disease, which is diagnosed in approximately 1/3,100 [73], 1/1,250 [74], and 1/7,000 [75, 76] neonates in Italy, Taiwan, and Japan, respectively.

The early pediatric, clinical features of FD are neuropathic pain, anhidrosis, angiokeratoma, and/or cornea verticillate [77]. Neurological involvement, common in adult patients with FD, leads to a wide variety of signs and symptoms, including headache, vertigo/dizziness, transient ischemic attacks, and ischemic strokes. A large, retrospective study of FD patients ($n = 2446$) found that 6.9% of male and 4.3% of female patients with a mean age of 39.0 and 45.7 years, respectively, experienced a stroke [78]. Moreover, patients with stroke had a high prevalence of hypertension, cardiac disease, and renal disease [78].

In FD, both large and small vessels are affected by cerebral vasculopathy. Researchers hypothesize that endothelial dysfunction, cerebral hyperperfusion, a prothrombotic state, and increased synthesis of reactive oxygen species contribute to the vascular dysfunction [79] Additionally, smooth muscle proliferation in the arterial media layer, atherosclerosis, and the initiation of an inflammatory cascade in the vessel wall can worsen vasculopathy in FD [80].

Neuroimaging of FD reveals a variety of features ranging from small vessel ischemia, ischemic stroke (including those secondary to cardiac involvement), and hypertensive hemorrhage (including those secondary to renal involvement) to vertebrobasilar artery dolichoectasia (Fig. 8) [77, 81–83]. Deep white matter lesions caused by small vessel ischemia are common in FD even in the absence of neurological symptoms. An accumulation of small vessel ischemia contributes to cognitive decline [84]. Although rare, children and adolescents with FD may present with non-hemorrhagic white matter and deep gray matter lesions alone without any clinical history of stroke [85, 86]. Infarctions in the posterior circulation and vertebrobasilar dolichoectasia reportedly occur at a higher frequency in FD [87, 88].

The pulvinar sign is defined as symmetric or asymmetric hyperintensity in the pulvinar nuclei on T1-weighted imaging. Initially thought to be pathognomonic of the disease, its actual incidence was recently calculated at approximately 3% of FD cases, which is significantly lower than previously thought [89]. Its pathogenesis is still unclear, although the hypothesis that it is caused by subtle, dystrophic calcification stemming from chronic hypoperfusion secondary to microvascular alterations is now widely accepted.

Other lysosomal storage disorders

Cerebral arteriopathy has recently been recognized as a feature of other lysosomal storage disorders (LSDs), such as mucopolysaccharidosis (MPS) and Pompe disease.

Mucopolysaccharidoses, a group of inherited LSDs stemming from an accumulation of glycosaminoglycans (GAGs), impact multiple systems. MPS I (Hurler syndrome, OMIM #607,014 and Scheie syndrome, OMIM #607,016) and MPS II (Hunter syndrome, OMIM #309,900) with acute ischemic stroke are the two known types although the number of documented cases is small [90–95]. The disease affects individuals from late infancy to young adulthood, and the infarct occurs in the corona radiata, posterior limb of the internal capsule, and middle cerebral arterial (MCA) territory. Multiple conditions associated with GAG accumulation may contribute to increasing the risk of stroke. Valvular thickening and fibrosis may result in cardiac thrombosis [96]. Severe hydrocephalus may compress the cerebral arteries. Progressive, sclerotic vasculopathy in an MPS I canine model was found to share the morphological and molecular features of massive, eccentric, luminal "plaques" of proteoglycans, collagen, myofibroblasts, vascular smooth muscle cells, and CD68 + activated macrophages with atherosclerosis [97]. Additionally, GAGs and GAG-derived oligosaccharides were found to initiate a pro-inflammatory signaling cascade culminating in macrophage activation via toll-like receptor 4 (TLR4) and its downstream mediator, activated nuclear factor-B (NF-B) [98]. However, more studies are needed to explain the etiology of cerebrovascular arteriopathy in MPS.

Pompe disease (glycogen storage disease type II, OMIM #232,300) is an autosomal recessive LSD characterized by abnormal glycogen accumulation within lysosomes. It is a multisystem disorder involving the heart, skeletal muscle, and liver. Cardiomyopathy and hypotonia are the defining characteristics of infantile-onset Pompe disease (IOPD) whereas involvement of skeletal muscle and respiratory insufficiency predominates in late-onset Pompe disease (LOPD) [99]. Glycogen deposition is found in the neurons of the cerebral cortex, brainstem, and anterior horn of the spinal cord, as well as in the glial cells of the cerebral cortex and the Purkinje cells of the cerebellum [100–102]. Additionally, glycogen deposition also occurs in the peripheral nervous system and smooth muscle of the tunica media of the cerebral arteries [103, 104]. ERT has markedly prolonged efficacy in IOPD but cannot cross the blood–brain barrier; it has also led to the discovery of secondary features of the disease, including white matter abnormalities, subtle signal abnormalities in the basal ganglia and brainstem, and ventricular dilatation in the CNS [105–108]. Brain changes may be the direct result of the glycogen deposition and delayed myelination [105, 108]. Microangiopathies (e.g., white matter lesions, microbleeds, ischemic stroke) and macro-angiopathies (e.g. dolichoectasia, aneurysms, and restrictive arteriopathy mostly of the vertebrobasilar

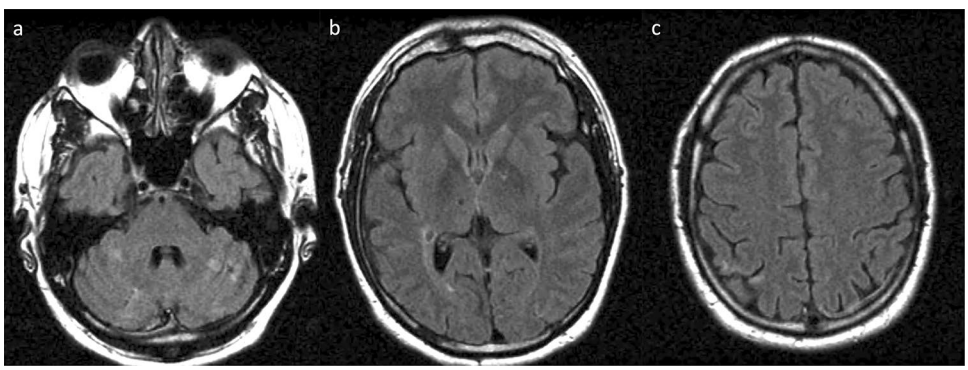

Fig. 8 Fabry disease in a 35-year-old, male patient with a history of headache. **a–c** Axial FLAIR imaging demonstrated multiple, small, old infarcts in the cerebral cortices, deep gray matter, deep white matter, and cerebellar hemisphere

arteries) occur relatively frequently in LOPD [109–113]. Bright tongue sign, an abnormal, diffuse T1 hyperintensity of the tongue musculature, is also common in LOPD [114]. While rare, vertebrobasilar dilative cerebral arteriopathy has also been reported in IOPD [106, 115].

Cystathionine β-synthase deficiency (CBSD) ("classic" homocystinuria)

Cystathionine β-synthase deficiency (CBSD, OMIM #236,200), or classic homocystinuria, is an autosomal recessive disorder caused by mutations in the *CBS* gene at 21q22. CBSD impairs cystathionine synthesis and increases homocysteine, methionine, and other metabolites. The eye (ectopia lentis and/or severe myopia), skeletal system (excessive height, long limbs, scoliosis, and pectus excavatum), vascular system (thromboembolism), and CNS (developmental delay/intellectual disability, psychiatric problems, seizures, and/or extrapyramidal signs) are affected [116]. Homocysteine increases superoxide and hydrogen peroxide, coagulation factor, and arterial smooth muscle cell proliferation [117]. Hypercoagulability-related, thromboembolic events can induce occlusive peripheral venous and arterial disorders, cerebrovascular events, and myocardial infarctions, increasing morbidity and death. Hypermethioninemia can serve as a clue to diagnosing CBSD in newborn screening.

Neuroimaging studies usually reveal several, minor brain infarcts at different ages (Fig. 9) [118]. Secondary venous infarction may result from dural sinus thrombosis [119]. Diffuse signal intensity in the white matter and increased intracranial pressure can result from hypermethioninemia-induced demyelination, white matter vacuolization, and spongy degeneration [120, 121]. MR angiography (MRA) and MR venography (MRV) may help identify large cerebral artery and intracranial dural sinus occlusion, and T2-weighted MRI may demonstrate intraocular lens displacement, another sign of CBSD.

5,10-Methylene-tetrahydrofolate reductase deficiency (MTHFRD)

5,10-Methylene-tetrahydrofolate reductase deficiency (MTHFRD, OMIM #236,250) is a common inborn error of folate metabolism. It is an autosomal recessive disorder caused by mutations in the *MTHFR* gene, which encodes an enzyme that converts homocysteine to methionine in the remethylation pathway. Thus, MTHFRD causes hyperhomocysteinemia and hypomethioninemia. MTHFRD frequently presents in childhood with gait abnormalities, seizures, and psychomotor impairment [122].

MTHFRD is related to an S-adenosylmethionine (SAM) deficit in the CSF and brain and spinal cord demyelination [123]. *MTHFR* mutations, including a minor form (*C677T* polymorphism), increase the risk of childhood stroke and cervical artery dissection [124]. Patients with MTHFRD should not receive nitrous gas as an anesthetic because it may induce methionine synthase deficiency, which may interact with the hereditary defect in *MTHFR* to cause neurological deterioration and death [125].

In children and adults with MTHFRD, MRI demonstrates white matter abnormalities ranging from small foci to more widespread regions of high signal intensity indicating demyelination (Fig. 10) [121, 126]. Venous thrombosis, cerebral microbleeds, and vascular infarction may also be present [127]. The dorsal and lateral spinal cord columns may be demyelinated [128]. White matter choline (cho) and N-acetylaspartate (NAA) peak levels on ^{1}H-MRS are slightly decreased [129, 130]. Decreased cho is probably

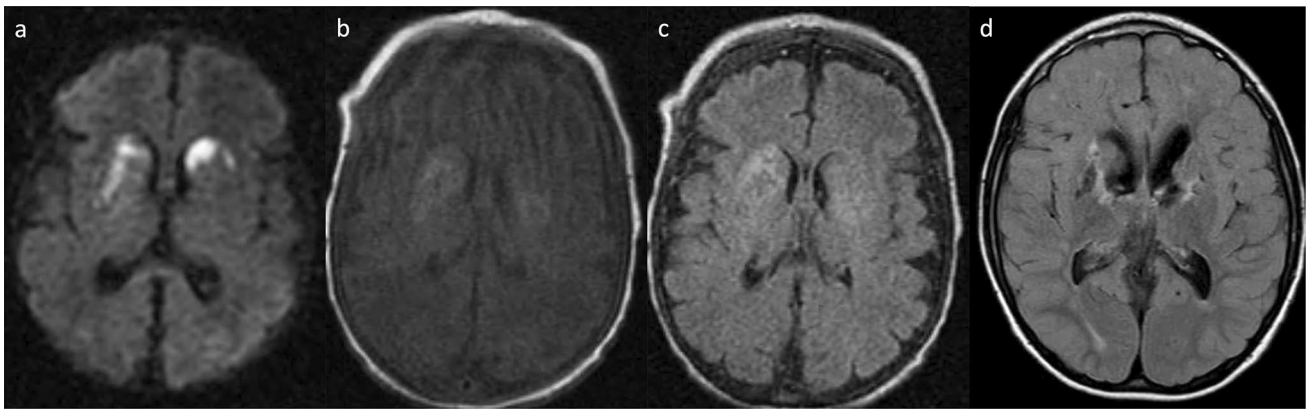

Fig. 9 Cystathionine β-synthase deficiency (CBSD) and methylmalonic acidemia in a male neonate with seizure. Axial DWI (**a**) revealed hyperintense lesions in the bilateral caudate nuclei and putamina. Axial T1-weighted imaging (**b**) and FLAIR (**c**) imaging demonstrated mild swelling and hyperintensity in the right caudate nucleus, bilateral putamina, and left globus pallidus indicating necrosis. Follow-up axial FLAIR imaging (**d**) at the age of 9 years found multiple, old infarcts in the bilateral basal ganglia and white matter volume loss

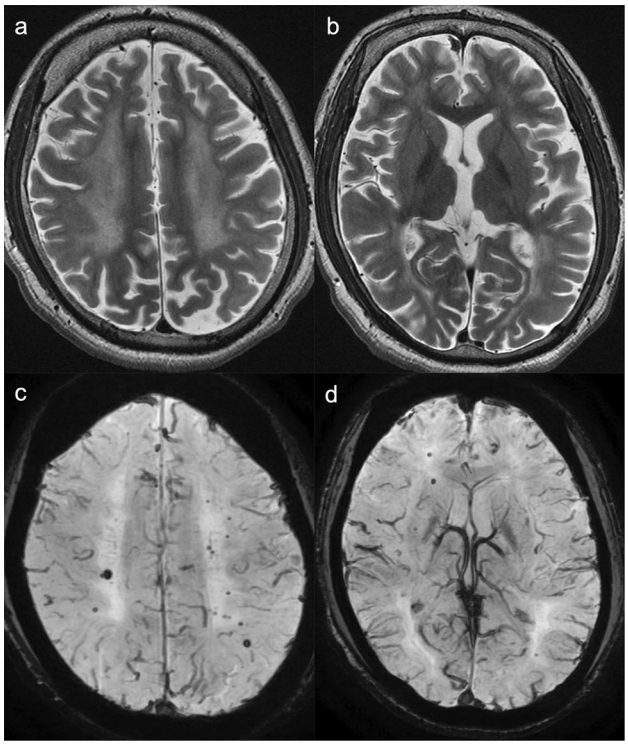

Fig. 10 5,10-methylene-tetrahydrofolate reductase deficiency (MTHFRD) in an 18-year-old, male patient with epilepsy, intellectual disability, and an autistic tendency. The patient had lower limb motor weakness and urinary incontinence for 4 years. **a**, **b** Axial T2-weighted imaging demonstrated mild brain atrophy and white matter hyperintensities with posterior predominance. **c**, **d** Axial SWAN demonstrated multiple, cerebral microbleeds in the white matter (reprinted with permission from Reference [121]). SWAN, T2 star-weighted MR angiography

secondary to the depletion of labile methyl groups produced by the transmethylation pathway.

Leukoencephalopathy with calcifications and cysts (LCC)

Leukoencephalopathy with calcifications and cysts (LCC; also known as Labrune syndrome, OMIM #614,561) is a rare, autosomal recessive disorder caused by biallelic mutations in small nucleolar RNA, C/D Box 118 (*SNORD118*), a non-protein-coding, small nucleolar RNA gene on chromosome 17p13 [131, 132]. The clinical presentation of LCC includes slowing of cognitive performance, convulsive seizures (rarely), and a mix of extrapyramidal, cerebellar, and pyramidal signs [133]. Its clinical onset ranges from early infancy to late adulthood. Female patients are slightly more numerous, and the majority of cases are diagnosed in children and young adults [134].

LCC is characterized by a triad of neuroimaging findings, including diffuse and asymmetric leukoencephalopathy, extensive calcification, and parenchymal brain cysts

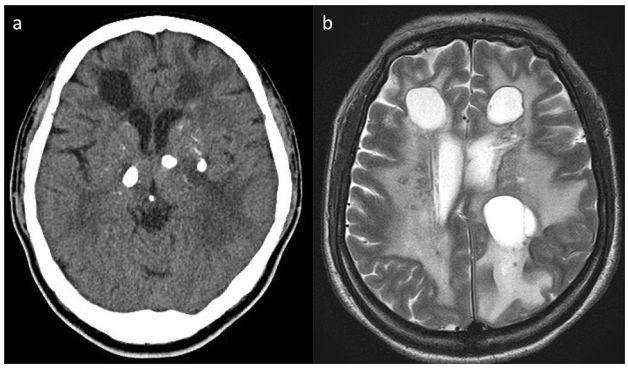

Fig. 11 Leukoencephalopathy with calcifications and cysts (LCC) in a 45-year-old, female patient with headache, cognitive decline, spasticity, and speech disturbance. **a** Axial non-contrast computed tomography revealed multiple, asymmetrical calcifications in the bilateral basal ganglia, thalami, and subcortical white matter and cyst formation in the bilateral, frontal white matter. **b** T2-weighted imaging demonstrated multiple, giant cysts and leukoencephalopathy, along with multiple, punctate hypointensities reflecting the calcifications in the bilateral white matter (this case was provided by professor Junichi Takanashi of Tokyo Women's Medical University, Yachiyo Medical Center)

(Fig. 11). CT and MR imaging demonstrate increased white matter signal intensity sparing the U-fibers and corpus callosum, with extensive, coarse calcification of the basal ganglia, brain stem, and subcortical white matter. Ring-like enhancement along the cyst wall or nodular enhancement in the degenerated white matter indicates disruption of the blood–brain barrier (BBB) and angiogenesis [134, 135]. DWI reveals increased diffusion in the cysts and surrounding white matter, indicating excessive water content. ^{1}H-MRS of the cysts demonstrates only the lactate peak but no brain metabolites [135], indicating energy failure in the cyst wall parenchyma. Furthermore, Wang et al. reported reduced NAA and cho in the leukoencephalic lesions [136].

Histopathological examination reveals vascular, tumor-like hyperplasia, Rosenthal fibers, glial proliferation, calcification, hyperplasia of the vessel wall, necrosis, degeneration, iron deposition, demyelination, vascular inflammatory changes, thrombosis, and hemorrhage [133–135].

The neuroimaging features of LCC are similar to those of cerebroretinal microangiopathy with calcifications and cysts (CRMCC, OMIM #612,199), also known as Coats plus syndrome. In contrast to LCC, CRMCC is also characterized by extraneurological, systemic lesions, such as bilateral retinal telangiectasias and exudations, intrauterine growth retardation, skeletal and hematological abnormalities, recurrent gastrointestinal hemorrhage, sparse hair, and dysplastic nails. Although LCC and CRMCC were initially thought to be manifestations of the same disorder, recessively inherited compound heterozygous mutations in the *CTC1* gene have

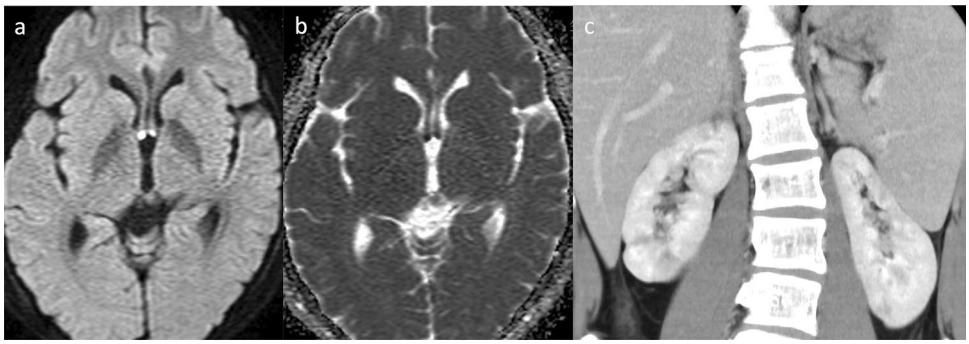

Fig. 12 Deficiency of adenosine deaminase type 2 (DADA2) in a male patient aged 18 years who received the diagnosis of DADA2 at the same time as his older brother (this patient has already been reported by Nihira et al. "P3" corresponds to this case). [142] Axial DWI (**a**) and ADC map (**b**) exhibited diffusion restriction in the bilateral column of the fornix, leading to the diagnosis of fornix infarction. The patient experienced memory loss spanning 2–3 days prior to MRI imaging. MR angiography found no stenosis in the major branches (not shown). Contrast-enhanced computed tomography (**c**) demonstrated impaired renal cortical enhancement and irregularities suggestive of a previous renal infarction. Additionally, splenomegaly was observed

been identified in CRMCC patients, suggesting that these two disorders are not allelic [137, 138].

Deficiency of adenosine deaminase type 2 (DADA2)

Deficiency of adenosine deaminase type 2 (DADA2, OMIM #615,688) is an autosomal recessive disorder caused by a mutation in the *ADA2* gene (previously known as *CECR1*) on chromosome 22q11. ADA2 is a dimeric, extracellular enzyme primarily secreted by myeloid lineage cells that converts adenosine to inosine. In addition to its catalytic function, ADA2 is thought to possess anti-inflammatory and immunomodulatory properties and to contribute to the maintenance of vascular integrity [139].

DADA2 usually presents in childhood. Most patients exhibit symptoms of a systemic, vascular, inflammatory disorder, including skin ulceration and recurrent strokes, which lead to neurological dysfunction. Additional characteristics may include recurrent fever, elevated acute-phase proteins, myalgia, lesions resembling polyarteritis nodosa, and/or livedo racemosa or reticularis with inflammatory vasculitis on biopsy. Some patients may exhibit renal and/or gastrointestinal involvement, hypertension, aneurysm formation, ischemic necrosis of the digits or clinical immunodeficiency. The hematological manifestations may sometimes resemble Diamond-Blackfan anemia [140].

CNS involvement resulting from small- and medium-sized vessel vasculopathy is a well-recognized complication occurring in approximately 50% of cases [141]. Neuroimaging features of DAD2 are multiple, recurrent, acute or chronic lacunar ischemic infarcts located in the deep brain nuclei and/or the brainstem (Fig. 12) [142–144], hemorrhagic stroke, intracranial bleeding (Fig. 13) [142–144], and spinal infarcts [143]. MR angiography may reveal an aneurysm or stenosis in the medium-sized arteries [143, 144]. Peculiar, probably inflammatory, perivascular tissue in the basal and prepontine cisterns may also be observed [143]. Peripheral neuropathy, acute sensorineural hearing loss, optic neuritis, and other ophthalmological abnormalities may also occur.

Anti-tumor necrosis factor (TNF) agents are recommended as a treatment for both symptomatic and asymptomatic DAD2 as they prevent or eliminate manifestations of autoinflammatory disease and vasculitis, reduce the risk of ischemic stroke, reduce the inflammatory burden, and ameliorate immunodeficiency, hepatosplenomegaly, and neutropenia [140]. HSCT has been shown to be curative for DADA2 [145].

Conclusion

The present review discussed the clinical and neuroimaging features of monogenic cSVD, which occurs from the prenatal to adolescent stage of development. A multidisciplinary approach involving pediatric neurologists, geneticists, and neuroradiologists is essential for accurate diagnosis, comprehensive monitoring, and tailored management of monogenic cSVD. Advancing our understanding of these disorders is essential for improving clinical outcomes in affected individuals.

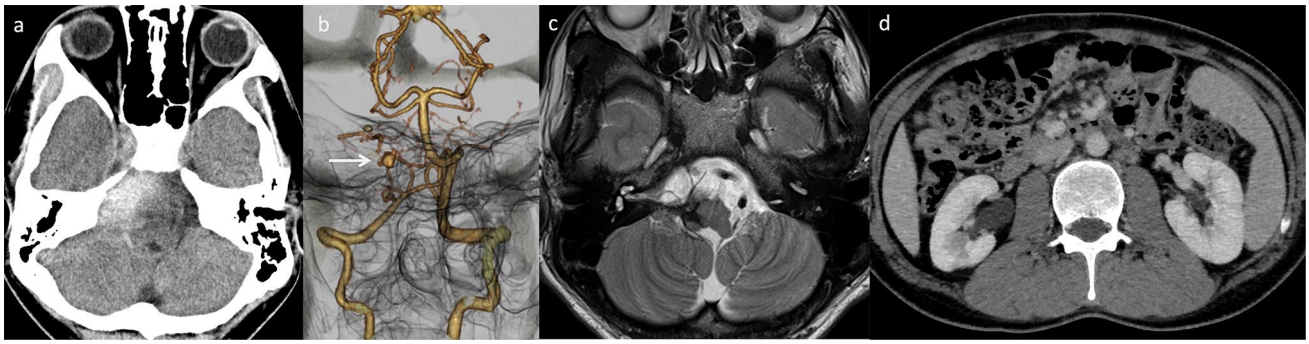

Fig. 13 A 26-year-old, male patient, the sibling of the patient mentioned above (Fig. 12), with deficiency of adenosine deaminase type 2 (DADA2). He had a history of recurrent diplopia, sensory numbness, and right-sided hearing impairment since the age of approximately 10 years. His cutaneous symptoms consisted of rash (livedo racemosa) and a history of frostbite. At the age of 22 years, DADA2 caused by defective ADA2 activity in the plasma was diagnosed (this patient has already been reported by Nihira et al. "P2" corresponds to this case) [142]. **a** Initial head non-contrast computed tomography (CT) revealed a parenchymal hemorrhage on the right side of the pons and a subarachnoid hemorrhage along the prepontine cistern. **b** Subsequent CT angiography indicated a possible pseudoaneurysm of the right anterior inferior cerebellar artery (AICA) (arrow). **c** Follow-up T2-weighted imaging demonstrated hemosiderin deposition around the brainstem region, suggesting previous, hemorrhagic events. **d** Contrast-enhanced CT highlighted impaired renal cortical enhancement and irregularities suggestive of a previous renal infarction. Splenomegaly was also observed

Acknowledgements We thank Mr. James Robert Valera for his assistance with editing this manuscript.

Funding None.

Declarations

Conflict of interest The authors declare that they have no conflicts of interest.

Ethical approval This article does not contain any studies involving human subjects or animals performed by any of the authors.

References

1. Li Q, Yang Y, Reis C, Tao T, Li W, Li X, et al. Cerebral small vessel disease. Cell Transplant. 2018;27:1711–22.
2. Pantoni L. Cerebral small vessel disease: from pathogenesis and clinical characteristics to therapeutic challenges. Lancet Neurol. 2010;9:689–701.
3. Wardlaw JM, Smith EE, Biessels GJ, Cordonnier C, Fazekas F, Frayne R, et al. Neuroimaging standards for research into small vessel disease and its contribution to ageing and neurodegeneration. Lancet Neurol. 2013;12:822–38.
4. Muñoz Maniega S, Chappell FM, Valdés Hernández MC, Armitage PA, Makin SD, Heye AK, et al. Integrity of normal-appearing white matter: Influence of age, visible lesion burden and hypertension in patients with small-vessel disease. J Cereb Blood Flow Metab. 2017;37:644–56.
5. Baykara E, Gesierich B, Adam R, Tuladhar AM, Biesbroek JM, Koek HL, et al. A novel imaging marker for small vessel disease based on skeletonization of white matter tracts and diffusion histograms. Ann Neurol. 2016;80:581–92.
6. Duering M, Righart R, Wollenweber FA, Zietemann V, Gesierich B, Dichgans M. Acute infarcts cause focal thinning in remote cortex via degeneration of connecting fiber tracts. Neurology. 2015;84:1685–92.
7. Duering M, Finsterwalder S, Baykara E, Tuladhar AM, Gesierich B, Konieczny MJ, et al. Free water determines diffusion alterations and clinical status in cerebral small vessel disease. Alzheimers Dement. 2018;14:764–74.
8. Debette S, Schilling S, Duperron M-G, Larsson SC, Markus HS. Clinical significance of magnetic resonance imaging markers of vascular brain injury: a systematic review and meta-analysis. JAMA Neurol. 2019;76:81–94.
9. Bos D, Wolters FJ, Darweesh SKL, Vernooij MW, de Wolf F, Ikram MA, et al. Cerebral small vessel disease and the risk of dementia: a systematic review and meta-analysis of population-based evidence. Alzheimers Dement. 2018;14:1482–92.
10. Whittaker E, Thrippleton S, Chong LYW, Collins VG, Ferguson AC, Henshall DE, et al. Systematic review of cerebral phenotypes associated with monogenic cerebral small-vessel disease. J Am Heart Assoc. 2022;11: e025629.
11. Yamamoto Y, Craggs L, Baumann M, Kalimo H, Kalaria RN. Review: molecular genetics and pathology of hereditary small vessel diseases of the brain. Neuropathol Appl Neurobiol. 2011;37:94–113.
12. Ilinca A, Englund E, Samuelsson S, Truvé K, Kafantari E, Martinez-Majander N, et al. MAP3K6 mutations in a neurovascular disease causing stroke, cognitive impairment, and tremor. Neurol Genet [Internet]. 2021 [cited 2023 Apr 4];7. https://ng.neurology.org/content/7/1/e548.

13. Ilinca A, Samuelsson S, Piccinelli P, Soller M, Kristoffersson U, Lindgren AG. A stroke gene panel for whole-exome sequencing. Eur J Hum Genet. 2019;27:317–24.
14. Marini S, Anderson CD, Rosand J. Genetics of cerebral small vessel disease. Stroke. 2020;51:12–20.
15. Persyn E, Hanscombe KB, Howson JMM, Lewis CM, Traylor M, Markus HS. Genome-wide association study of MRI markers of cerebral small vessel disease in 42,310 participants. Nat Commun. 2020;11:2175.
16. Chabriat H, Joutel A, Dichgans M, Tournier-Lasserve E, Bousser M-G. CADASIL. Lancet Neurol. 2009;8:643–53.
17. Khoshnoodi J, Pedchenko V, Hudson BG. Mammalian collagen IV. Microsc Res Tech. 2008;71:357–70.
18. Meuwissen MEC, Halley DJJ, Smit LS, Lequin MH, Cobben JM, de Coo R, et al. The expanding phenotype of COL4A1 and COL4A2 mutations: clinical data on 13 newly identified families and a review of the literature. Genet Med. 2015;17:843–53.
19. Jeanne M, Gould DB. Genotype-phenotype correlations in pathology caused by collagen type IV alpha 1 and 2 mutations. Matrix Biol. 2017;57–58:29–44.
20. Maurice P, Guilbaud L, Garel J, Mine M, Dugas A, Friszer S, et al. Prevalence of COL4A1 and COL4A2 mutations in severe fetal multifocal hemorrhagic and/or ischemic cerebral lesions. Ultrasound Obstet Gynecol. 2021;57:783–9.
21. Gould DB, Phalan FC, Breedveld GJ, van Mil SE, Smith RS, Schimenti JC, et al. Mutations in Col4a1 cause perinatal cerebral hemorrhage and porencephaly. Science. 2005;308:1167–71.
22. George E, Vassar R, Mogga A, Li Y, Norton ME, Gano D, et al. Spectrum of fetal intraparenchymal hemorrhage in COL4A1/A2-related disorders. Pediatr Neurol. 2023;147:63–7.
23. Yoneda Y, Haginoya K, Kato M, Osaka H, Yokochi K, Arai H, et al. Phenotypic spectrum of COL4A1 mutations: porencephaly to schizencephaly. Ann Neurol. 2013;73:48–57.
24. Cavallin M, Mine M, Philbert M, Boddaert N, Lepage JM, Coste T, et al. Further refinement of COL4A1 and COL4A2 related cortical malformations. Eur J Med Genet. 2018;61:765–72.
25. Niwa T, Aida N, Osaka H, Wada T, Saitsu H, Imai Y. Intracranial hemorrhage and tortuosity of veins detected on susceptibility-weighted imaging of a child with a type IV Collagen α1 mutation and schizencephaly. Magn Reson Med Sci. 2015;14:223–6.
26. Guey S, Hervé D. Main features of COL4A1-COL4A2 related cerebral microangiopathies. Cereb Circul Cognit Behav. 2022;3:100140.
27. Shah S, Ellard S, Kneen R, Lim M, Osborne N, Rankin J, et al. Childhood presentation of COL4A1 mutations. Dev Med Child Neurol. 2012;54:569–74.
28. Itai T, Miyatake S, Taguri M, Nozaki F, Ohta M, Osaka H, et al. Prenatal clinical manifestations in individuals with COL4A1/2 variants. J Med Genet. 2021;58:505–13.
29. Vahedi K, Alamowitch S. Clinical spectrum of type IV collagen (COL4A1) mutations: a novel genetic multisystem disease. Curr Opin Neurol. 2011;24:63–8.
30. Plaisier E, Gribouval O, Alamowitch S, Mougenot B, Prost C, Verpont MC, et al. COL4A1 mutations and hereditary angiopathy, nephropathy, aneurysms, and muscle cramps. N Engl J Med. 2007;357:2687–95.
31. Mancuso M, Arnold M, Bersano A, Burlina A, Chabriat H, Debette S, et al. Monogenic cerebral small-vessel diseases: diagnosis and therapy. Consensus recommendations of the European Academy of Neurology. Eur J Neurol. 2020;27:909–27.
32. Gould DB, Phalan FC, van Mil SE, Sundberg JP, Vahedi K, Massin P, et al. Role of COL4A1 in small-vessel disease and hemorrhagic stroke. N Engl J Med. 2006;354:1489–96.
33. Mochida GH, Ganesh VS, Felie JM, Gleason D, Hill RS, Clapham KR, et al. A homozygous mutation in the tight-junction protein JAM3 causes hemorrhagic destruction of the brain, subependymal calcification, and congenital cataracts. Am J Hum Genet. 2010;87:882–9.
34. Akawi NA, Canpolat FE, White SM, Quilis-Esquerra J, Morales Sanchez M, Gamundi MJ, et al. Delineation of the clinical, molecular and cellular aspects of novel JAM3 mutations underlying the autosomal recessive hemorrhagic destruction of the brain, subependymal calcification, and congenital cataracts. Hum Mutat. 2013;34:498–505.
35. Miyatake S, Schneeberger S, Koyama N, Yokochi K, Ohmura K, Shiina M, et al. Biallelic COLGALT1 variants are associated with cerebral small vessel disease. Ann Neurol. 2018;84:843–53.
36. Teunissen MWA, Kamsteeg E-J, Sallevelt SCE, Pennings M, Bauer NJC, Jeroen Vermeulen R, et al. Biallelic variants in the COLGALT1 gene causes severe congenital porencephaly. Neurol Genet. 2021;7(2):e564.
37. Smahi A, Courtois G, Rabia SH, Döffinger R, Bodemer C, Munnich A, et al. The NF-kappaB signalling pathway in human diseases: from incontinentia pigmenti to ectodermal dysplasias and immune-deficiency syndromes. Hum Mol Genet. 2002;11:2371–5.
38. Fusco F, Fimiani G, Tadini G, D'urso M, Ursini MV. Clinical diagnosis of incontinentia pigmenti in a cohort of male patients. J Am Acad Dermatol. 2007;56:264–7.
39. Scheuerle AE, Ursini MV. Incontinentia pigmenti. Seattle: University of Washington; 2017.
40. Tomotaki S, Shibasaki J, Yunoki Y, Kishigami M, Imagawa T, Aida N, et al. Effectiveness of corticosteroid therapy for acute neurological symptoms in incontinentia pigmenti. Pediatr Neurol. 2016;56:55–8.
41. Rr P, Douch C, Aan Koh MJ, Lai AHM, Lim CT, Hartley L, et al. Speckled brain lesions in incontinentia pigmenti patients with acquired brain syndromes. Eur J Paediatr Neurol. 2021;33:106–11.
42. Kanai S, Okanishi T, Kawai M, Yoshino G, Tsubouchi Y, Nishimura Y, et al. Late-onset cerebral arteriopathy in a patient with incontinentia pigmenti. Brain Dev. 2021;43:580–4.
43. Meuwissen MEC, Mancini GMS. Neurological findings in incontinentia pigmenti; a review. Eur J Med Genet. 2012;55:323–31.
44. Maingay-de Groof F, Lequin MH, Roofthooft DW, Oranje AP, de Coo IF, Bok LA, et al. Extensive cerebral infarction in the newborn due to incontinentia pigmenti. Eur J Paediatr Neurol. 2008;12:284–9.
45. Minić S, Trpinac D, Obradović M. Systematic review of central nervous system anomalies in incontinentia pigmenti. Orphanet J Rare Dis. 2013;8:25.
46. Soltirovska Salamon A, Lichtenbelt K, Cowan FM, Casaer A, Dudink J, Dereymaeker A, et al. Clinical presentation and spectrum of neuroimaging findings in newborn infants with incontinentia pigmenti. Dev Med Child Neurol. 2016;58:1076–84.
47. Hadj-Rabia S, Froidevaux D, Bodak N, Hamel-Teillac D, Smahi A, Touil Y, et al. Clinical study of 40 cases of incontinentia pigmenti. Arch Dermatol. 2003;139:1163–70.
48. Phan TA, Wargon O, Turner AM. Incontinentia pigmenti case series: clinical spectrum of incontinentia pigmenti in 53 female patients and their relatives. Clin Exp Dermatol. 2005;30:474–80.
49. Crow YJ. Aicardi-Goutières Syndrome. Seattle: University of Washington; 2016.
50. Crow YJ, Manel N. Aicardi-Goutières syndrome and the type I interferonopathies. Nat Rev Immunol. 2015;15:429–40.
51. Rice GI, Forte GMA, Szynkiewicz M, Chase DS, Aeby A, Abdel-Hamid MS, et al. Assessment of interferon-related biomarkers in Aicardi-Goutières syndrome associated with mutations in TREX1, RNASEH2A, RNASEH2B, RNASEH2C, SAMHD1, and ADAR: a case-control study. Lancet Neurol. 2013;12:1159–69.

52. Livingston JH, Crow YJ. Neurologic phenotypes associated with mutations in TREX1, RNASEH2A, RNASEH2B, RNASEH2C, SAMHD1, ADAR1, and IFIH1: Aicardi-Goutières syndrome and beyond. Neuropediatrics. 2016;47:355–60.
53. La Piana R, Uggetti C, Roncarolo F, Vanderver A, Olivieri I, Tonduti D, et al. Neuroradiologic patterns and novel imaging findings in Aicardi-Goutières syndrome. Neurology. 2016;86:28–35.
54. Nunes RH, Pacheco FT, da Rocha AJ. Magnetic resonance imaging of anterior temporal lobe cysts in children: discriminating special imaging features in a particular group of diseases. Neuroradiology. 2014;56:569–77.
55. Ramesh V, Bernardi B, Stafa A, Garone C, Franzoni E, Abinun M, et al. Intracerebral large artery disease in Aicardi-Goutières syndrome implicates SAMHD1 in vascular homeostasis. Dev Med Child Neurol. 2010;52:725–32.
56. Livingston JH, Lin J-P, Dale RC, Gill D, Brogan P, Munnich A, et al. A type I interferon signature identifies bilateral striatal necrosis due to mutations in ADAR1. J Med Genet. 2014;51:76–82.
57. Kameli R, Amanat M, Rezaei Z, Hosseionpour S, Nikbakht S, Alizadeh H, et al. RNASET2-deficient leukoencephalopathy mimicking congenital CMV infection and Aicardi-Goutieres syndrome: a case report with a novel pathogenic variant. Orphanet J Rare Dis. 2019;14:184.
58. Cetin Gedik K, Lamot L, Romano M, Demirkaya E, Piskin D, Torreggiani S, et al. The 2021 European Alliance of Associations for Rheumatology/American College of Rheumatology points to consider for diagnosis and management of autoinflammatory type I interferonopathies: CANDLE/PRAAS, SAVI, and AGS. Arthritis Rheumatol. 2022;74:735–51.
59. Vanderver A, Adang L, Gavazzi F, McDonald K, Helman G, Frank DB, et al. Janus Kinase Inhibition in the Aicardi-Goutières Syndrome. N Engl J Med. 2020;383:986–9.
60. Munnich A, Rustin P. Clinical spectrum and diagnosis of mitochondrial disorders. Am J Med Genet. 2001;106:4–17.
61. Iizuka T, Sakai F. Pathogenesis of stroke-like episodes in MELAS: analysis of neurovascular cellular mechanisms. Curr Neurovasc Res. 2005;2:29–45.
62. Kim IO, Kim JH, Kim WS, Hwang YS, Yeon KM, Han MC. Mitochondrial myopathy-encephalopathy-lactic acidosis-and strokelike episodes (MELAS) syndrome: CT and MR findings in seven children. AJR Am J Roentgenol. 1996;166:641–5.
63. Yonemura K, Hasegawa Y, Kimura K, Minematsu K, Yamaguchi T. Diffusion-weighted MR imaging in a case of mitochondrial myopathy, encephalopathy, lactic acidosis, and stroke like episodes. AJNR Am J Neuroradiol. 2001;22:269–72.
64. Majoie CB, Akkerman EM, Blank C, Barth PG, Poll-The BT, den Heeten GJ. Mitochondrial encephalomyopathy: comparison of conventional mr imaging with diffusion-weighted and diffusion tensor imaging: case report. AJNR Am J Neuroradiol. 2002;23:813–6.
65. Oppenheim C, Galanaud D, Samson Y, Sahel M, Dormont D, Wechsler B, et al. Can diffusion weighted magnetic resonance imaging help differentiate stroke from stroke-like events in MELAS? J Neurol Neurosurg Psychiatry. 2000;69:248–50.
66. Bhatia KD, Krishnan P, Kortman H, Klostranec J, Krings T. Acute cortical lesions in MELAS syndrome: anatomic distribution, symmetry, and evolution. AJNR Am J Neuroradiol. 2020;41:167–73.
67. Mitani T, Aida N, Tomiyasu M, Wada T, Osaka H. Transient ischemic attack-like episodes without stroke-like lesions in MELAS. Pediatr Radiol. 2013;43:1400–3.
68. Tsujikawa T, Yoneda M, Shimizu Y, Uematsu H, Toyooka M, Ikawa M, et al. Pathophysiologic evaluation of MELAS strokes by serially quantified MRS and CASL perfusion images. Brain Dev. 2010;32:143–9.
69. Minobe S, Matsuda A, Mitsuhashi T, Ishikawa M, Nishimura Y, Shibata K, et al. Vasodilatation of multiple cerebral arteries in early stage of stroke-like episode with MELAS. J Clin Neurosci. 2015;22:407–8.
70. Li R, Xiao H-F, Lyu J-H, Wang JJD, Ma L, Lou X. Differential diagnosis of mitochondrial encephalopathy with lactic acidosis and stroke-like episodes (MELAS) and ischemic stroke using 3D pseudocontinuous arterial spin labeling. J Magn Reson Imaging. 2017;45:199–206.
71. Ikawa M, Yoneda M, Muramatsu T, Matsunaga A, Tsujikawa T, Yamamoto T, et al. Detection of preclinically latent hyperperfusion due to stroke-like episodes by arterial spin-labeling perfusion MRI in MELAS patients. Mitochondrion. 2013;13:676–80.
72. Ashley GA, Shabbeer J, Yasuda M, Eng CM, Desnick RJ. Fabry disease: twenty novel α-galactosidase A mutations causing the classical phenotype. J Hum Genet. 2001;46:192–6.
73. Spada M, Pagliardini S, Yasuda M, Tukel T, Thiagarajan G, Sakuraba H, et al. High incidence of later-onset Fabry disease revealed by newborn screening. Am J Hum Genet. 2006;79:31–40.
74. Hwu W-L, Chien Y-H, Lee N-C, Chiang S-C, Dobrovolny R, Huang A-C, et al. Newborn screening for Fabry disease in Taiwan reveals a high incidence of the later-onset GLA mutation c.936+919G>A (IVS4+919G>A). Hum Mutat. 2009;30:1397–405.
75. Inoue T, Hattori K, Ihara K, Ishii A, Nakamura K, Hirose S. Newborn screening for Fabry disease in Japan: prevalence and genotypes of Fabry disease in a pilot study. J Hum Genet. 2013;58:548–52.
76. Sawada T, Kido J, Yoshida S, Sugawara K, Momosaki K, Inoue T, et al. Newborn screening for Fabry disease in the western region of Japan. Mol Genet Metab Rep. 2020;22: 100562.
77. Germain DP. Fabry disease. Orphanet J Rare Dis. 2010;5:30.
78. Sims K, Politei J, Banikazemi M, Lee P. Stroke in Fabry disease frequently occurs before diagnosis and in the absence of other clinical events: natural history data from the Fabry Registry. Stroke. 2009;40:788–94.
79. Moore DF, Kaneski CR, Askari H, Schiffmann R. The cerebral vasculopathy of Fabry disease. J Neurol Sci. 2007;257:258–63.
80. Mishra V, Banerjee A, Gandhi AB, Kaleem I, Alexander J, Hisbulla M, et al. Stroke and Fabry disease: a review of literature. Cureus. 2020;12: e12083.
81. Cocozza S, Russo C, Pontillo G, Pisani A, Brunetti A. Neuroimaging in Fabry disease: current knowledge and future directions. Insights Imaging. 2018;9:1077–88.
82. Fellgiebel A, Müller MJ, Ginsberg L. CNS manifestations of Fabry's disease. Lancet Neurol. 2006;5:791–5.
83. Søndergaard CB, Nielsen JE, Hansen CK, Christensen H. Hereditary cerebral small vessel disease and stroke. Clin Neurol Neurosurg. 2017;155:45–57.
84. Okeda R, Nisihara M. An autopsy case of Fabry disease with neuropathological investigation of the pathogenesis of associated dementia. Neuropathology. 2008;28:532–40.
85. Marchesoni C, Cisneros E, Pfister P, Yáñez P, Rollan C, Romero C, et al. Brain MRI findings in children and adolescents with Fabry disease. J Neurol Sci. 2018;395:131–4.
86. Cabrera-Salazar MA, O'Rourke E, Charria-Ortiz G, Barranger JA. Radiological evidence of early cerebral microvascular disease in young children with Fabry disease. J Pediatr. 2005;147:102–5.
87. Rolfs A, Böttcher T, Zschiesche M, Morris P, Winchester B, Bauer P, et al. Prevalence of Fabry disease in patients with cryptogenic stroke: a prospective study. Lancet. 2005;366:1794–6.
88. Baptista MV, Ferreira S, Pinho-E-Melo T, Carvalho M, Cruz VT, Carmona C, et al. Mutations of the GLA gene in young patients with stroke: the PORTYSTROKE study–screening

genetic conditions in Portuguese young stroke patients. Stroke. 2010;41:431–6.
89. Cocozza S, Russo C, Pisani A, Olivo G, Riccio E, Cervo A, et al. Redefining the Pulvinar sign in Fabry disease. AJNR Am J Neuroradiol. 2017;38:2264–9.
90. Grant N, Taylor JM, Plummer Z, Myers K, Burrow T, Luchtman-Jones L, et al. Case report: cerebral revascularization in a child with mucopolysaccharidosis Type I. Front Pediatr. 2021;9: 606905.
91. Olgaç A. Acute stroke in A patient with mucopolysaccharidosis type 1 with increased carotis intima media thickness. Eurasian J Med Oncol [Internet]. 2018. https://doi.org/10.14744/ejmo.2018.51523.
92. Fujii D, Manabe Y, Tanaka T, Kono S, Sakai Y, Narai H, et al. Scheie syndrome diagnosed after cerebral infarction. J Stroke Cerebrovasc Dis. 2012;21:330–2.
93. Kimura M, Azuma Y, Taguchi S, Takagi M, Mori H, Shimomura Y, et al. Subcortical infarction in a young adult with Hunter syndrome. Brain Dev. 2022;44:343–6.
94. Sharma K, Cummock J, Maertens P. Acute arterial ischemic stroke in a treated child with Hunter's syndrome: a case report and review of the literature. J Pediatr Neurol. 2021;19:069–75.
95. Neely J, Carpenter J, Hsu W, Jordan L, Restrepo L. Cerebral infarction in Hunter syndrome. J Clin Neurosci. 2006;13:1054–7.
96. Braunlin E, Orchard PJ, Whitley CB, Schroeder L, Reed RC, Manivel JC. Unexpected coronary artery findings in mucopolysaccharidosis. Report of four cases and literature review. Cardiovasc Pathol. 2014;23:145–51.
97. Lyons JA, Dickson PI, Wall JS, Passage MB, Ellinwood NM, Kakkis ED, et al. Arterial pathology in canine mucopolysaccharidosis-I and response to therapy. Lab Invest. 2011;91:665–74.
98. Wang RY, Braunlin EA, Rudser KD, Dengel DR, Metzig AM, Covault KK, et al. Carotid intima-media thickness is increased in patients with treated mucopolysaccharidosis types I and II, and correlates with arterial stiffness. Mol Genet Metab. 2014;111:128–32.
99. Leslie N, Bailey L. Pompe Disease. Seattle: University of Washington; 2017.
100. Gambetti P, DiMauro S, Baker L. Nervous system in Pompe's disease. Ultrastructure and biochemistry. J Neuropathol Exp Neurol. 1971;30:412–30.
101. Pena LDM, Proia AD, Kishnani PS. Postmortem Findings and Clinical Correlates in Individuals with Infantile-Onset Pompe Disease. JIMD Rep. 2015;23:45–54.
102. Sakurai I, Tosaka A, Mori Y, Imura S, Aoki K. Glycogenosis type II (Pompe). The fourth autopsy case in Japan. Acta Pathol Jpn. 1974;24:829–46.
103. Kretzschmar HA, Wagner H, Hübner G, Danek A, Witt TN, Mehraein P. Aneurysms and vacuolar degeneration of cerebral arteries in late-onset acid maltase deficiency. J Neurol Sci. 1990;98:169–83.
104. Thurberg BL, Lynch Maloney C, Vaccaro C, Afonso K, Tsai AC-H, Bossen E, et al. Characterization of pre- and post-treatment pathology after enzyme replacement therapy for Pompe disease. Lab Invest. 2006;86:1208–20.
105. Chien Y-H, Lee N-C, Peng S-F, Hwu W-L. Brain development in infantile-onset Pompe disease treated by enzyme replacement therapy. Pediatr Res. 2006;60:349–52.
106. McIntosh PT, Hobson-Webb LD, Kazi ZB, Prater SN, Banugaria SG, Austin S, et al. Neuroimaging findings in infantile Pompe patients treated with enzyme replacement therapy. Mol Genet Metab. 2018;123:85–91.
107. Ebbink BJ, Poelman E, Aarsen FK, Plug I, Régal L, Muentjes C, et al. Classic infantile Pompe patients approaching adulthood: a cohort study on consequences for the brain. Dev Med Child Neurol. 2018;60:579–86.
108. Paoletti M, Pichiecchio A, Colafati GS, Conte G, Deodato F, Gasperini S, et al. Multicentric retrospective evaluation of five classic infantile Pompe disease subjects under enzyme replacement therapy with early infratentorial involvement. Front Neurol. 2020;11: 569153.
109. Montagnese F, Granata F, Musumeci O, Rodolico C, Mondello S, Barca E, et al. Intracranial arterial abnormalities in patients with late onset Pompe disease (LOPD). J Inherit Metab Dis. 2016;39:391–8.
110. Sandhu D, Rizvi A, Kim J, Reshi R. Diffuse cerebral microhemorrhages in a patient with adult-onset Pompe's disease: a case report. J Vasc Interv Neurol. 2014;7:82–5.
111. Hossain MA, Miyajima T, Akiyama K, Eto Y. A case of adult-onset Pompe disease with cerebral stroke and left ventricular hypertrophy. J Stroke Cerebrovasc Dis. 2018;27:3046–52.
112. Huded V, Bohra V, Prajapati J, DeSouza R, Ramankutty R. Stroke in young-dilative arteriopathy: a clue to late-onset Pompe's disease? J Stroke Cerebrovasc Dis. 2016;25:e50–2.
113. Malhotra K, Carrington DC, Liebeskind DS. Restrictive arteriopathy in late-onset Pompe disease: case report and review of the literature. J Stroke Cerebrovasc Dis. 2017;26:e172–5.
114. Karam C, Dimitrova D, Yutan E, Chahin N. Bright tongue sign in patients with late-onset Pompe disease. J Neurol. 2019;266:2518–23.
115. Viamonte M, Tuna I, Rees J. Dilated cerebral arteriopathy in classical Pompe disease: a novel finding. Pediatr Neurol. 2020;108:117–20.
116. Morris AAM, Kožich V, Santra S, Andria G, Ben-Omran TIM, Chakrapani AB, et al. Guidelines for the diagnosis and management of cystathionine beta-synthase deficiency. J Inherit Metab Dis. 2017;40:49–74.
117. Peterson JC, Spence JD. Vitamins and progression of atherosclerosis in hyper-homocyst(e)inaemia. Lancet. 1998;351:263.
118. Ruano MM, Castillo M, Thompson JE. MR imaging in a patient with homocystinuria. AJR Am J Roentgenol. 1998;171:1147–9.
119. Buoni S, Molinelli M, Mariottini A, Rango C, Medaglini S, Pieri S, et al. Homocystinuria with transverse sinus thrombosis. J Child Neurol. 2001;16:688–90.
120. Brenton JN, Matsumoto JA, Rust RS, Wilson WG. White matter changes in an untreated, newly diagnosed case of classical homocystinuria. J Child Neurol. 2014;29:88–92.
121. Enokizono M, Aida N, Yagishita A, Nakata Y, Ideguchi R, Kurokawa R, et al. Neuroimaging findings of inborn errors of metabolism: urea cycle disorders, aminoacidopathies, and organic acidopathies. Jpn J Radiol. 2023;41:683–702.
122. Huemer M, Mulder-Bleile R, Burda P, Froese DS, Suormala T, Zeev BB, et al. Clinical pattern, mutations and in vitro residual activity in 33 patients with severe 5, 10 methylenetetrahydrofolate reductase (MTHFR) deficiency. J Inherit Metab Dis. 2016;39:115–24.
123. Surtees R, Leonard J, Austin S. Association of demyelination with deficiency of cerebrospinal-fluid S-adenosylmethionine in inborn errors of methyl-transfer pathway. Lancet. 1991;338:1550–4.
124. Pezzini A, Del Zotto E, Archetti S, Negrini R, Bani P, Albertini A, et al. Plasma homocysteine concentration, C677T MTHFR genotype, and 844ins68bp CBS genotype in young adults with spontaneous cervical artery dissection and atherothrombotic stroke. Stroke. 2002;33:664–9.
125. Selzer RR, Rosenblatt DS, Laxova R, Hogan K. Adverse effect of nitrous oxide in a child with 5,10-methylenetetrahydrofolate reductase deficiency. N Engl J Med. 2003;349:45–50.
126. van den Berg M, van der Knaap MS, Boers GH, Stehouwer CD, Rauwerda JA, Valk J. Hyperhomocysteinaemia; with reference to its neuroradiological aspects. Neuroradiology. 1995;37:403–11.

127. Grow JL, Fliman PJ, Pipe SW. Neonatal sinovenous thrombosis associated with homozygous thermolabile methylenetetrahydrofolate reductase in both mother and infant. J Perinatol. 2002;22:175–8.
128. Hao M, Zhang Y, Hou S, Chen Y, Shi M, Zhao G, et al. Spinal cord demyelination combined with hyperhomocysteinemia: a case report. Neuropsychiatr Dis Treat. 2014;10:2057–9.
129. Debray F-G, Boulanger Y, Khiat A, Decarie J-C, Orquin J, Roy M-S, et al. Reduced brain choline in homocystinuria due to remethylation defects. Neurology. 2008;71:44–9.
130. Engelbrecht V, Rassek M, Huismann J, Wendel U. MR and proton MR spectroscopy of the brain in hyperhomocysteinemia caused by methylenetetrahydrofolate reductase deficiency. AJNR Am J Neuroradiol. 1997;18:536–9.
131. Jenkinson EM, Rodero MP, Kasher PR, Uggenti C, Oojageer A, Goosey LC, et al. Mutations in SNORD118 cause the cerebral microangiopathy leukoencephalopathy with calcifications and cysts. Nat Genet. 2016;48:1185–92.
132. Iwama K, Mizuguchi T, Takanashi J-I, Shibayama H, Shichiji M, Ito S, et al. Identification of novel SNORD118 mutations in seven patients with leukoencephalopathy with brain calcifications and cysts. Clin Genet. 2017;92:180–7.
133. Labrune P, Lacroix C, Goutières F, de Laveaucoupet J, Chevalier P, Zerah M, et al. Extensive brain calcifications, leukodystrophy, and formation of parenchymal cysts: a new progressive disorder due to diffuse cerebral microangiopathy. Neurology. 1996;46:1297–301.
134. Ma Y, Zhang X, Cheng C, Xu Q, Di H, Zhao J, et al. Leukoencephalopathy with calcifications and cysts: a case report. Medicine. 2017;96: e7597.
135. Sener U, Zorlu Y, Men S, Bayol U, Zanapalioglu U. Leukoencephalopathy, cerebral calcifications, and cysts. AJNR Am J Neuroradiol. 2006;27:200–3.
136. Wang M, Zhang M, Wu L, Dong Z, Yu S. Leukoencephalopathy with cerebral calcification and cysts: cases report and literature review. J Neurol Sci. 2016;370:173–9.
137. Anderson BH, Kasher PR, Mayer J, Szynkiewicz M, Jenkinson EM, Bhaskar SS, et al. Mutations in CTC1, encoding conserved telomere maintenance component 1, cause Coats plus. Nat Genet. 2012;44:338–42.
138. Polvi A, Linnankivi T, Kivelä T, Herva R, Keating JP, Mäkitie O, et al. Mutations in CTC1, encoding the CTS telomere maintenance complex component 1, cause cerebroretinal microangiopathy with calcifications and cysts. Am J Hum Genet. 2012;90:540–9.
139. Zhou Q, Yang D, Ombrello AK, Zavialov AV, Toro C, Zavialov AV, et al. Early-onset stroke and vasculopathy associated with mutations in ADA2. N Engl J Med. 2014;370:911–20.
140. Aksentijevich I, Moura NS, Barron K. Adenosine deaminase 2 deficiency. Seattle: University of Washington; 2019.
141. Fayand A, Sarrabay G, Belot A, Hentgen V, Kone-Paut I, Grateau G, et al. Multiple facets of ADA2 deficiency: Vasculitis, autoinflammatory disease and immunodeficiency: a literature review of 135 cases from literature. Rev Med Internet. 2018;39:297–306.
142. Nihira H, Izawa K, Ito M, Umebayashi H, Okano T, Kajikawa S, et al. Detailed analysis of Japanese patients with adenosine deaminase 2 deficiency reveals characteristic elevation of type II interferon signature and STAT1 hyperactivation. J Allergy Clin Immunol. 2021;148:550–62.
143. Geraldo AF, Caorsi R, Tortora D, Gandolfo C, Ammendola R, Alessio M, et al. Widening the neuroimaging features of adenosine deaminase 2 deficiency. AJNR Am J Neuroradiol. 2021;42:975–9.
144. Bulut E, Erden A, Karadag O, Oguz KK, Ozen S. Deficiency of adenosine deaminase 2; special focus on central nervous system imaging. J Neuroradiol. 2019;46:193–8.
145. Hashem H, Kumar AR, Müller I, Babor F, Bredius R, Dalal J, et al. Hematopoietic stem cell transplantation rescues the hematological, immunological, and vascular phenotype in DADA2. Blood. 2017;130:2682–8.